17th Australasian Fluid Mechanics Conference
Auckland, New Zealand
5-9 December 2010

Development of a CFD model for an oscillating hydrofoil

S. R. Hutchison[1], P. A. Brandner[1], J. R. Binns[1] A. D. Henderson[2] and G. J. Walker[2]

[1]The National Centre For Maritime and Hydrodynamics, Australian Maritime College
University of Tasmania, Launceston, Tasmania, 7250, Australia

[2]School of Engineering
University of Tasmania, Hobart, Tasmania, 7001, Australia

Abstract

Unsteady two-dimensional flow about an oscillating hydrofoil is investigated computationally as a preparatory stage for three dimensional fluid structure interaction studies. A dynamically deformed mesh at static incidence angles was used to assess grid independence in preparation for unsteady runs. The computation used a high resolution advection scheme with a shear stress transport turbulence model. Validation was conducted using steady and dynamic experimental results. Lift coefficients normalised for all pitch oscillations to fall on to a single phase trajectory at reduced frequencies of 0.78, 1.57 and 3.14.

Introduction

The motivation of the present analyses is to investigate the hydroelastic response of marine propellers. These often operate in an unsteady wake region generated by the hull and control surfaces. This causes the propeller to be subjected to unsteady loading [26]. In this investigation the propeller problem has been simplified to a single hydrofoil response to an oscillation in pure pitch indicative of the propeller passing through the wake deficits generated by control surfaces. Hydroelasticity is a multidisciplinary study of dynamics, elastics and fluid dynamics [3, 12]. This study investigates a rigid two-dimensional (2D) oscillating foil in pure pitch. The effectiveness of ANSYS CFX to predict unsteady dynamics of attached flow up to and including 10° incidence with no cavitation is also evaluated. Reduced frequency is defined as $k=\omega c/2U_\infty$ where ω=circular frequency, c=chord and U_∞=free stream velocity.

NASA in the late 1970s and early 1980s conducted a number of experiments into dynamic stall and unsteady loading of airfoils [1, 2, 11, 14, 15, 18]. These studies obtained lift, drag and pitching moment measurements by integrating surface pressures. They also investigated boundary layer transition, separation and reattachment characteristics, as well as flow reversal and chordwise unsteady pressures. McCroskey et. al [19] found that in general, unsteady motion is more important than airfoil shape when determining dynamic stall characteristics. In 1982 McCroskey and Pucci[18] conducted ten specific experiments on foil sections NACA 0012, Vertol VR-7 and NLR-7301 undergoing oscillations to evaluate unsteady viscous theories and computation methods. McCroskey et al.[18, 17] identified four distinct regimes of viscous-inviscid interactions corresponding to varying degrees of unsteady flow separation. If a foil oscillates with a maximum incidence angle (α) below static stall angle, the boundary layer on both upper and lower surfaces will remain fully attached, except for a small separation bubble near the upper surface on the leading edge for $\alpha<5°$, which produces transition from laminar to turbulent flow. Koochesfahani [13] demonstrated experimentally that thrust production for a foil due to pitching motions occurs only above certain reduced frequencies. He also found that the structure of the wake can be substantially modified by amplitude of oscillation, frequency and shape of the wave form. In 1993 Piziali [20] conducted a comprehensive set of experiments investigating the pressure distributions on a foil undergoing pitching motions for 2D and three-dimensional (3D) airfoils for the development of computational and empirical methods. In 1994 Hart [10] investigated experimentally unsteady flow induced by periodic change of incidence. These experiments provided details of the change in boundary layer profile on the suction and pressure sides and phase lag for 2D and 3D hydrofoils for varying *k*.

Analytical solutions of note include: formulae for thrust/drag force for an airfoil in heaving and pitching motion [8]; forces, moments and phase angles for a thin flat plate in an incompressible fluid with a trailing vorticity sheet as a function of *k* [24, 25]; and defining fluid dynamic behavior by *k*.

McCroskey [16] conducted some of the earliest numerical investigations. He developed simple formulas to describe the detailed inviscid, incompressible flow field of an unsteady airfoil with thickness and camber. The next detailed numerical analyses were conducted to investigate the use of k-ε and Shear Stress Transport (SST) k-ω models for predicting dynamic stall [5, 6]. It was generally observed that none of the turbulence models could predict the hysteresis effect during the downstroke. It has been shown that upwind-biased schemes, even though more computationally intensive, provide an improved solution of unsteady flows because they have no dependence on the specified numerical dissipation parameters and they appear to have less grid sensitivity compared with central difference schemes [5]. More recently a series of numerical simulations of dynamic stall for 3D foils using various planform shapes were completed providing detailed information on the interaction of dynamic stall and the tip vortex [21, 22, 23].

Methodology

Steady state and dynamic numerical analyses were conducted. Steady state was used to determine boundary layer resolution and a comparison with experimental steady state forces. The computed boundary layer properties for steady flow were compared with XFOIL [4] predictions and published experimental data [9]. A displacement diffusion mesh deformation model was used to deform the mesh to the required incidence. Dynamic validation was conducted against experimental results contained in [20], which used 2° oscillation amplitude ($\Delta\alpha$) in pure pitch around a mean incidence (α_m) of 4°, Reynolds number($Re_c = U_\infty c/\nu$) of $1.98\text{x}10^6$ and a pitch center at 1/4 chord(c) for a NACA 0015. Oscillating hydrofoil studies of a NACA0009 were conducted for $\Delta\alpha$ of 2, 5 and 10° at α_m 0° and pitch center at 1/2c.

CFD Setup

The unsteady flow field was solved with the commercially available package ANSYS CFX version 12.1 with a 2D one layer deep structured mesh consisting of hexahedral elements. The inlet had specified velocity components and an isotropic turbu-

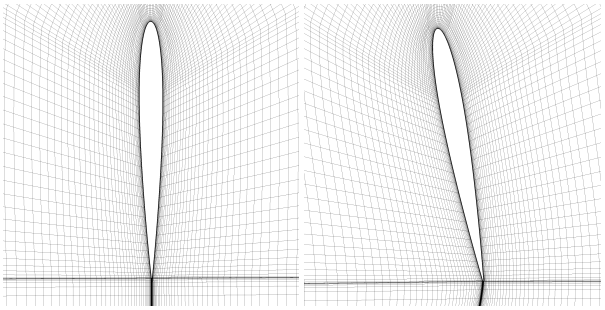

(a) undeformed α=0° (b) deformed α=10°

Figure 1: C-grid topology for NACA 0009

lence intensity of 0.5% and the length scale is calculated within ANSYS to account for varying levels of turbulence. The domain outlet had constant pressure with zero gradient turbulence. The boundaries either side of the foil in the spanwise direction were symmetric. The foil was moved dynamically with a specified displacement. The advection scheme used was the high resolution option for validation data; it was changed to a specific blend factor of 1 to make it second-order accurate [7] for the remaining dynamic analyses. A transient scheme of second order backward Euler convergence was used with a maximum of 10 internal calculating loops and a residual target of $1x10^{-4}$ max.

Grid Independence and Temporal Convergence

Grid independence and temporal convergence studies were conducted on the NACA 0009 and a similar mesh was then used to model the NACA 0012 and NACA 0015. A displacement diffusion mesh deformation model was used to generate the mesh for steady flow computations at 0, 2, 5 and 10° incidence Re_c of $2.8x10^6$ and $9.4x10^7$. It was found that a grid with 27284 elements had an average error of 0.2% using Richardson extrapolation. Figure 2 shows the temporal convergence plot. The resulting mesh was then used to assess time step convergence with a k of 0.25 and Re_c $2.8x10^6$. The temporal convergence of 100 time steps per period was selected to ensure the average Courant number on the foil remained less than 1 for the duration of one cycle. This resulted in a maximum Courant number of approximately 600 in the domain. All results were run out for 5 cycles, the first cycle contains transients from the steady start up solution and the second and the third cycle are identical.

Mesh Development

The structured grid was constructed using a C-topology within an H-topology at the trailing edge as shown in figure 1. The inlet velocity boundary is 2.5c upstream. The outlet pressure opening is 11.5c downstream. The first cell height was .02%c.

Validation

Gregory and O'Reilly [9] presented results for the distributions of the pressure coefficient C_P on a smooth NACA 0012 at a Re_c of $2.88x10^6$. Results from these experiments were compared with XFOIL and the k-ε, k-ω, and SST turbulence models, as shown in figure 3. Piziali [20] conducted a detailed series of oscillating wing aerodynamic tests with fast response pressure transducers. The lift, drag, and moment coefficients (C_L, C_D and C_M) were calculated from the pressure normal to the chord neglecting skin friction. The moment was calculated by integrating these pressures over the chord neglecting any moment due to the thickness of the foil. The three Reynolds Average Navier-Stokes models were compared with the experimental results of [20]. Results compared well for k values of 0.131 and 0.188 for all turbulence models. However, for the lower k of 0.038 using the k-ε and k-ω models and at a k of 0.093 using the k-ε model, for an Δα of 2 and 4° and a α_m of 4° the model was unstable. Although convergence was reached it had a large mean offset from the original data. The results compared well for all cases using the SST model. Results are presented for comparison for the case of Δα=2° and α_m=4°. A slight over estimate of C_L and underestimate for C_D was apparent in the upstroke, but the downstroke compared well for both C_L and C_D, (see figures 4 and 5). For C_M the results compared well on the upstroke but with the reversal of direction the change in the C_M slope is not as large as in experimental data figure 6. This resulted in a lower moment in the downstroke.

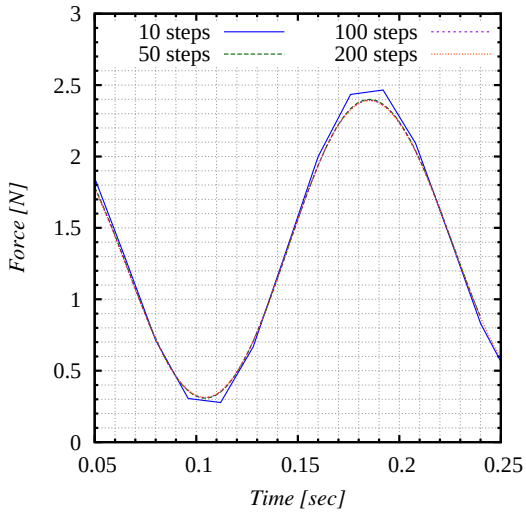

Figure 2: Temporal independence

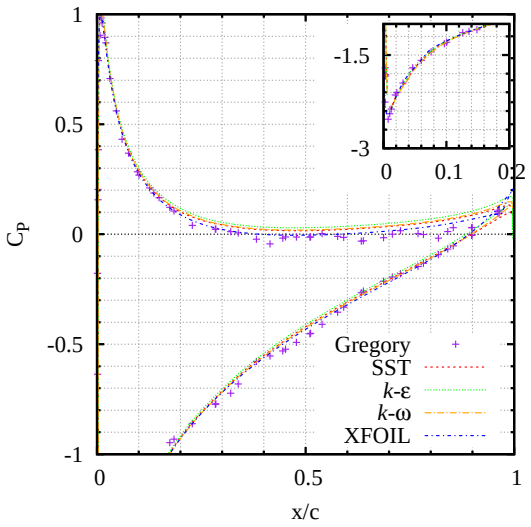

Figure 3: Comparison of computed and experimental chordwise pressure coefficients for a NACA 0012 α=6°

Results

The results were produced by rotating a NACA 0009 about a pitching axis at 1/2c. The test matrix variables consisted of α_m=0° Δα=2, 5 and 10° and Re_c=$2.8x10^6$ and $9.389x10^6$. It was found that there was no Re dependence for this matrix. All C_L phase trajectories were found to fall on one line when normalised by maximum incidence and the corresponding static lift

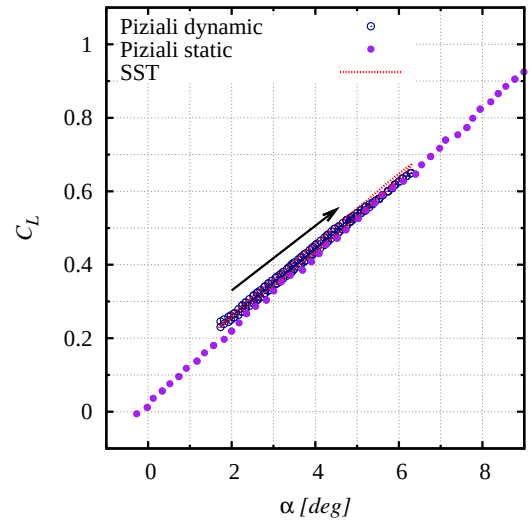

Figure 4: Comparison of computed and experimental C_L for a NACA 0015 at k=0.188, α_m=4°, and $\Delta\alpha$=2°

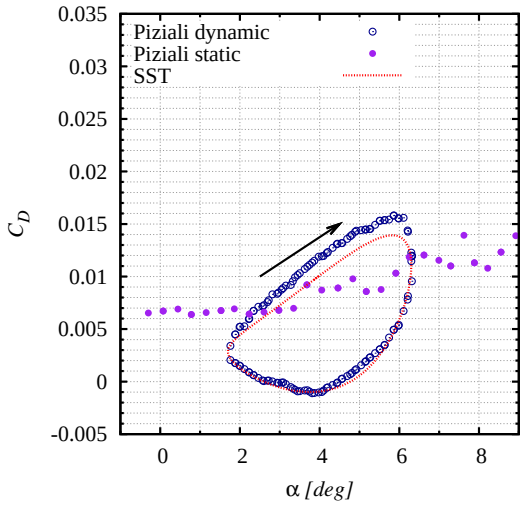

Figure 5: Comparison of computed and experimental C_D for a NACA 0015 at k=0.188, α_m=4°, and $\Delta\alpha$=2°

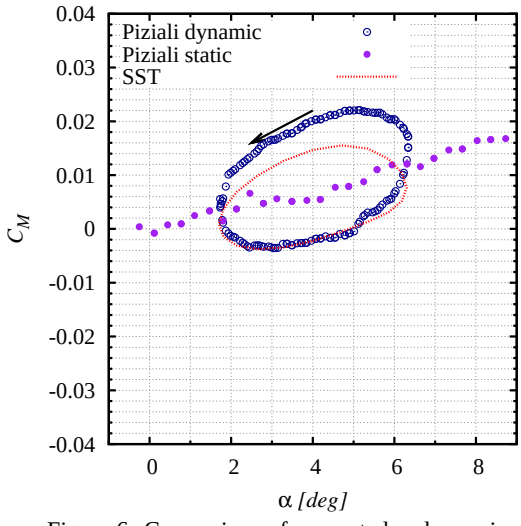

Figure 6: Comparison of computed and experimental C_M for a NACA 0015 at k=0.188, α_m=4°, and $\Delta\alpha$=2°

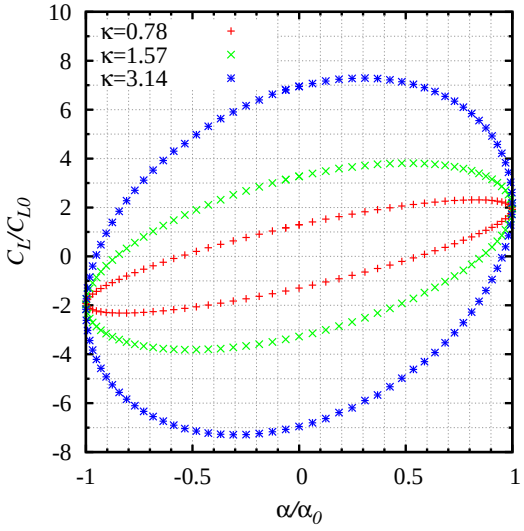

Figure 7: Effect of varying k on computed C_L/C_{L0} phase trajectory for varying k; for a NACA 0009 α_m=0° and $\Delta\alpha$=2°

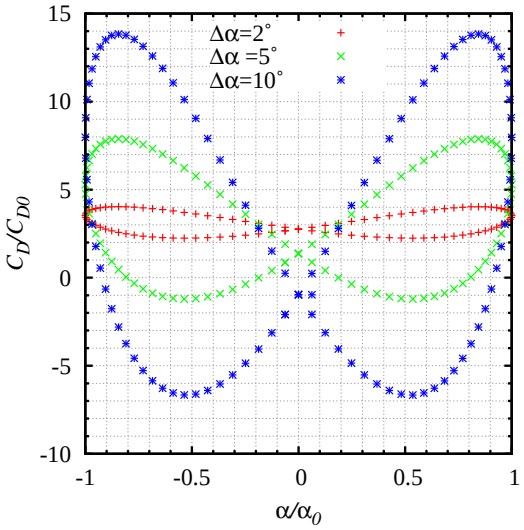

Figure 8: Effect of varying $\Delta\alpha$ on computed C_D/C_{D0} phase trajectory; for a NACA 0009, α_m=0° and k=0.785

coefficient C_{L0}, for each k, as shown figure 7. C_D and C_M do not however normalise in this manner. From figure 7 the phase lag is shown by the point at which the maximum C_L is reached on the hysteresis loop. It is noted that as k increases the phase lag becomes greater and the hysteresis loop becomes more circular. Figure 8 shows C_D to be symmetric about α_m=0° similar to static C_D. Both C_L and C_D lead the pitch oscillation in all cases. Figure 9 shows that C_M lags and opposes the pitching motion.

Conclusions

NACA 0009 and NACA 0015 profiles were investigated using a structured deforming grid. k-ε, k-ω and SST models were compared to Piziali [20] with the SST model using a high resolution advection scheme showing the closet comparison. This model compared well for C_L and C_D, but under-predicted C_M on the downstroke. Lift coefficients normalised for all pitch oscillations to fall on to a single phase trajectory at reduced frequencies of 0.78, 1.57 and 3.14.

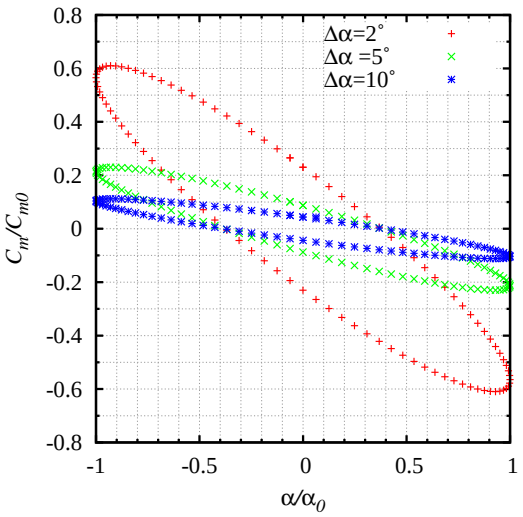

Figure 9: Effect of varying $\Delta\alpha$ on computed C_M/C_{M0} phase trajectory; for a NACA 0009, α_m=0° and k=0.785

Acknowledgments

This project is supported by The Australian Defence Science and Technology Organization (DSTO) and Australian Maritime College(AMC). The first author (SRH) is an Australian Postgraduate Award recipient.

References

[1] Carr, L. W., McAlister, K. W. and McCroskey, W. J., Analysis of the development of dynamic stall based on oscillating airfoil experiments, Technical Report A-6674; NASA-TN-D-8382, NACA, 1977.

[2] Carr, L. W., McCroskey, W. J., McAlister, K. W., Pucci, S. L. and Lambert, O., An experimental study of dynamic stall on advanced airfoil sections. volume 3: Hot-wire and hot film measurements, Technical Report TM-84245, NASA, 1982.

[3] Dowell, E., Clark, R., Cox, D., Curtiss, H., Edwards, J., Hall, K., Peters, D., Scanlan, R., Simiu, E., Sisto, F. and Strganax, T., *A modern course in aeroelasticity*, Kluwer Academic Publishers, Dordrecht/Boston/London, 2004, fourth edition.

[4] Drela, M. and Youngren, H., *XFOIL 6.9 User Primer*, MIT Aero and Astro and Aerocraft Inc., 2001.

[5] Ekaterinaris, J. A., Numerical investigation of dynamic stall of an oscillating wing, *AIAA Journal*, **33**, 1995, 5.

[6] Ekaterinaris, J. A. and Menter, F. R., Computation of oscillating airfoil flows with one and two equation turbulence models, *AIAA Journal*, **32**, 1994, 6.

[7] ANSYS Europe, *ANSYS CFX release Notes V12.1*, ANSYS Europe., 2009.

[8] Garrick, I. E., Propulsion of a flapping and oscillating airfoil, Technical Report TR-567, NACA, 1936.

[9] Gregory, N. and O'Reilly, C., Low-speed aerodynamic characteristics of naca 0012 aerofoil section, including effects of upper-surface roughness simulating hoar frost, Technical Report Reports and memoranda 3726, Ministry of Defence Aeronautical Research Council, 1973.

[10] Hart, D., Boundary layer formation on an oscillating hydrofoil, in *20th Symposium on Naval Hydrodynamics*, Santa Barbara, California, 1994, 187–197, 187–197.

[11] Hiliare, A. and Carta, F. O., Analysis of unswept and swept wing chordwise pressure data from an oscillating NACA 0012 airfoil experiment, Technical Report NASA-CR-3567, NASA, 1983.

[12] Hodges, D. H. and Pierce, G., *Introdutction to structural dynamics and aeroelasticity*, Kluwer Academic Publishers, Dordrecht/Boston/London, 2004, fourth edition.

[13] Koochesfahani, M. M., Vortical patterns in the wake of an oscillating airfoil, *AIAA Journal*, **27**, 1989, 1200-1205.

[14] McAlister, K. W., Carr, L. W. and McCroskey, J. W., Dynamic stall experiments on the NACA 0012 airfoil, Technical Report NACA TP-1100, NACA, 1978.

[15] McAlister, K. W., Pucci, S. L., McCroskey, W. J. and Carr, L. W., An experimental study of dynamic stall on advanced airfoil section. volume 2: Pressure and force data, Technical Report A-8925; NAS 1.15:84245-VOL-2; NASA-TM-84245-VOL-2; USAAVRADCOM-TR-82-A-8-VOL-2, 1982.

[16] McCroskey, W., Inviscid flowfield of an unsteady airfoil, *AIAA Journal*, **11**, 1973, 1130–1137.

[17] McCroskey, W., Unsteady airfoils, *Annual Review of Fluid Mechanics*, **14**, 1982, 285–311.

[18] McCroskey, W. and Pucci, S., Viscous-inviscid interaction on oscillating airfoils in subsonic flow, *AIAA Journal*, **20**, 1982, 167–174, AIAA 81-0051R.

[19] McCroskey, W. J., McAlister, K. W., Carr, L. W. and Pucci, S. L., An experimental study of dynamic stall on advanced airfoil sections. volume 1: Summary of the experiment, Technical Memorandum 84245, NASA, 1982.

[20] Piziali, R. A., An experimental investigation of 2d and 3d oscillating wing aerodynamics for a range of angle of attack including stall, NASA Technical Memorandum 4623.

[21] Spentzos, A., Barakos, G., Badcock, K., Richards, B., Wernert, P., Schreck, S. and Raffel, M., CFD investigation of 2d and 3d dynamic stall, in *AHS International 4th Decennial Specialists' Conference on Aeromechanics*, 2004.

[22] Spentzos, A., Barakos, G., Badcock, K., Richards, B., Wernert, P., Schreck, S. and Raffel, M., Investigation of three dimensional dynamic stall using computational fluid dynamics, *AIAA Journal*, **43**, 2005, 11.

[23] Spentzos, A., Barakos, G. N., Badcock, K. J., Richards, B. E., Coton, F. N., Galbraith, R. A. M., Berton, E. and Favier, D., Computational fluid dynamics study of three dimensional dynamic stall of various planform shapes, *Journal of Aircraft*, **44**, 2007, 10.

[24] Theodorsen, T., On the theory of wing sections with particular reference to the lift distribution, Report 383, NACA, 1930.

[25] vonK*árm*á*n*, T. and Sears, W., Airfoil theory for non-uniform motion, *Journal of the Aeronautical Sciences*, **5**, 1938, 379–390.

[26] Young, Y., Time-dependent hydroelastic analysis of cavitating propulsors, *Journal of Fluids and Structures*, **23**, 2007, 269–295.